Image Based Visual Servoing: Estimated Image Jacobian by Using Fundamental Matrix VS Analytic Jacobian

L. Pari[1], J.M. Sebastián[1], A. Traslosheros[1], and L. Angel[2]

[1] Departamento de Automática, Ingeniería Electrónica e Informática Industrial (DISAM)
Escuela Técnica Superior de Ingenieros Industriales, Universidad Politécnica de Madrid
C/ José Gutiérrez Abascal, 2, 28006 Madrid, Spain
[2] Facultad de Ingeniería Electrónica, Universidad Pontificia Bolivariana
Km. 7 Via de Piedecuesta, Bucaramanga, Colombia
{jsebas,lpari,atraslosheros,langel}@etsii.upm.es

Abstract. This paper describes a comparative study of performance between the estimated image Jacobian that come from taking into account the geometry epipolar of a system of two cameras, and the well known analytic image Jacobian that is utilized for most applications in visual servoing. Image Based Visual Servoing architecture is used for controlling a 3 d.o.f. articular system using two cameras in eye to hand configuration. Tests in static and dynamic cases were carried out, and showed that the performance of estimated Jacobian by using the properties of the epipolar geometry is such as good and robust against noise as the analytic Jacobian. This fact is considered as an advantage because the estimated Jacobian does not need laborious previous work prior the control task in contrast to the analytic Jacobian does.

Keywords: Visual servoing, Jacobian estimation, Fundamental matrix, Interaction matrix, robot Jacobian, positioning, tracking.

1 Introduction

Visual servoing consists in the use of visual information given by visual sensors (i.e. cameras) to control a robotic system. This kind of control turns out to be very useful in many applications because it allows us to know which objects are present in the scene with high accuracy, as well as their position, orientation and velocity. It makes possible to use robots in new domains where the workspace is not known a priori.

Among the existing classifications of visual servoing [4] [10] [11], one of the most known is the way that visual information is used to define the signal error to control the system [2]: Position Based Visual Servoing (PBVS) and the Image Based Visual Servoing (IBVS). In PBVS features are extracted from the image and used to reconstruct the 3D position of the target, whereas in IBVS the task is defined in the image plane directly through image features. In the latter a matrix is defined called the Image Jacobian, which linearly relates changes in image features and changes in Cartesian coordinates or changes in joints (in this case, it is called full-visual-motor Jacobian [1] [5] [11]).

Analytic Image Jacobian is widely used by the most researchers in Visual Servoing, it is well known that it require a thorough knowledge of the involved systems: calibration of the joint system, kinematic calibration of the vision system, and 3D reconstruction of features positions; they all are common sources of possible errors. In past papers [12] [15] we have presented a method to estimated image Jacobian by integrating epipolar geometry of the system [3], and compared with other existing algorithms from the literature with tests that consider static [12] and dynamic [15] cases.

In this paper, we have compared performance of the method that considers the epipolar geometry and the analytic Jacobian. Two kinds of tests have been also carried out, in the former a high number of positions into the workspace were reached, whereas in the latter, a high number of curve trajectories were tracked. Tests showed that robustness against noise obtained by the estimated Jacobian method that considers the epipolar geometry is also obtained by the analytic method. This fact is considered as an advantage, because the estimated method reaches good performance without the need of a laborious previous work to the task. In order to diversify the study, tests were extended to the recursive last square method which gave good results in past works [12] [15].

This paper is organized as follows: after the present introduction, section 2 details the terminology and theoretical concepts used in the paper. Sections 3 and 4 put forward the estimated and analytic Jacobian respectively. Section 5 describes the control law, whereas section 6 describes the applied workspace, tests, and results. Finally section 7 reflects our conclusion.

2 Image Jacobian

Assume that a robot or positioning system is observed from one or various fixed views. Let $\mathbf{r}=\begin{bmatrix} r_1 & r_2 & \cdots & r_p \end{bmatrix}^T$ be the p-dimensional vector that represents the position of the end effector in a Cartesian coordinate system. Let $\mathbf{q}=\begin{bmatrix} q_1 & q_2 & \cdots & q_n \end{bmatrix}^T$ be the n-dimensional vector that represents the joint position of the robot. Let $\mathbf{s}=\begin{bmatrix} s_1 & s_2 & \cdots & s_m \end{bmatrix}^T$ be the m-dimensional vector that represents the image features (for example the coordinates of a point in one or both images).

The relation between joint velocity of the robot $\dot{\mathbf{q}}=\begin{bmatrix} \dot{q}_1 & \dot{q}_2 & \cdots & \dot{q}_n \end{bmatrix}^T$ and its corresponding velocity in task space, $\dot{\mathbf{r}}=\begin{bmatrix} \dot{r}_1 & \dot{r}_2 & \cdots & \dot{r}_p \end{bmatrix}^T$, is captured in terms of the robot Jacobian, $\mathbf{J}_{rq}$, as $\dot{\mathbf{r}}=\mathbf{J}_{rq}\dot{\mathbf{q}}$. The relation between feature velocities $\dot{\mathbf{s}}=\begin{bmatrix} \dot{s}_1 & \dot{s}_2 & \cdots & \dot{s}_m \end{bmatrix}^T$ and task space velocities is given by $\dot{\mathbf{s}}=\mathbf{J}_{sr}\dot{\mathbf{r}}$, if the chosen feature is a point $\mathbf{s}=(u,v)^T$ in the image, and the Cartesian coordinates of the camera are used, $\mathbf{J}_{sr}$ is given by:

$$\mathbf{J}_{sr}=\begin{bmatrix} f/Z & 0 & -u/Z & -uv/f & \left(f^2+u^2\right)/f & -v \\ 0 & f/Z & -v/Z & -\left(f^2+u^2\right)/f & uv/f & u \end{bmatrix} \quad (1)$$

where u,v represent the central image coordinates, f is the focal distance, Z is the space coordinate of the point w.r.t. the camera coordinates, and $\dot{\mathbf{r}} = \begin{bmatrix} T_x & T_y & T_z & w_x & w_y & w_z \end{bmatrix}^T$ represents the translational and rotational speed of the point. Generally, $\mathbf{J}_{sr}$ is named as interaction matrix.

The velocity of the image features can be directly related to joint velocities in terms of a composite Jacobian named full-visual-motor Jacobian [5] [16]:

$$\dot{\mathbf{s}} = \mathbf{J}_{sq}\dot{\mathbf{q}} = \begin{bmatrix} \frac{\partial s_1}{\partial q_1} & \cdots & \frac{\partial s_1}{\partial q_n} \\ \vdots & \ddots & \vdots \\ \frac{\partial s_m}{\partial q_1} & \cdots & \frac{\partial s_m}{\partial qn} \end{bmatrix} \dot{\mathbf{q}} \quad ; \quad \text{where } \mathbf{J}_{sq} = \mathbf{J}_{sr}\mathbf{J}_{rq} = \mathbf{J} \tag{2}$$

Analytic Jacobian comes from, whereas estimated Jacobian from (2). It is necessary remark that to obtain the analytic Jacobian, there must be considered: the intrinsic parameters of the camera calibration (focal distance, image center coordinates), the 3D reconstruction of the point or an approximation (Z coordinate), the kinematic calibration of the camera (relation between camera coordinates and joint space origin), and the kinematic calibration of the robot. Most of previous works on visual servoing assume that the system structure and the system parameters are known, or the parameters can be identified in an off-line process. In contrast to estimate image Jacobian dynamically based on only changes in features and joints.

2.1 Multiple-View Jacobian

When several views are used, whether the interaction matrix or the full visual-motor Jacobian can be defined as the concatenation of the partial Jacobian for each view [1] [2] [15]. All the Jacobians share the same joint increments, although visual features are managed independently. In previous work [15], we carried out experiments comparing the results obtained using one of the cameras and those obtained using two cameras: our results showed that using two cameras instead of one improved the behaviour. In many applications, improvement in the performance more than justifies the possible disadvantages: increased equipment cost or calculation time.

3 Estimated Jacobian

3.1 Adding the epipolar constraint

Epipolar constraint (3) is taken into account in the calculation of the image Jacobian (2). If the considered visual features are centroids of points, and if we note a point in the first camera by ('), and in the second camera by ("), the projection of a 3D point on both images must satisfy the epipolar restriction equation:

$$\tilde{\mathbf{s}}''^T_k \mathbf{F} \tilde{\mathbf{s}}'_k = 0 \tag{3}$$

where features are expressed in projective notation (~), and **F** is a 3x3 matrix known as the fundamental matrix. Its knowledge is known as weak or projective calibration. A more detailed description can be found in [7] and [9].

Features at moments k and k-1 for each camera, is given by:

$$\tilde{\mathbf{s}}'_k = \tilde{\mathbf{s}}'_{k-1} + \tilde{\mathbf{J}}' \Delta\mathbf{q}_k \quad ; \quad \tilde{\mathbf{s}}''_k = \tilde{\mathbf{s}}''_{k-1} + \tilde{\mathbf{J}}'' \Delta\mathbf{q}_k \tag{4}$$

where $\Delta\mathbf{q}_k = \mathbf{q}_k - \mathbf{q}_{k-1}$, and $\tilde{\mathbf{J}}', \tilde{\mathbf{J}}''$ contain the variables to be solved that are elements of image Jacobian for each camera and have the form:

$$\tilde{\mathbf{J}}' = \begin{bmatrix} J'_{11} & J'_{12} & J'_{13} \\ J'_{21} & J'_{22} & J'_{23} \\ 0 & 0 & 0 \end{bmatrix} \text{ and } \tilde{\mathbf{J}}'' = \begin{bmatrix} J''_{11} & J''_{12} & J''_{13} \\ J''_{21} & J''_{22} & J''_{23} \\ 0 & 0 & 0 \end{bmatrix} \tag{5}$$

to do dimensionally correct equation (4).

Substituting (4) in (3), ordering terms and considering $\tilde{\mathbf{s}}''^{T}_{k-1} \mathbf{F} \tilde{\mathbf{s}}'_{k-1} = 0$, we have the following non-linear equation for $\tilde{\mathbf{J}}', \tilde{\mathbf{J}}''$ [12] [15]:

$$\Delta\mathbf{q}_k^T \tilde{\mathbf{J}}''^T \mathbf{F} \tilde{\mathbf{J}}' \Delta\mathbf{q}_k + \Delta\mathbf{q}_k^T \tilde{\mathbf{J}}''^T \mathbf{F} \tilde{\mathbf{s}}'_{k-1} + \tilde{\mathbf{s}}''^T_{k-1} \mathbf{F} \tilde{\mathbf{J}}' \Delta\mathbf{q}_k = 0 \tag{6}$$

Equation (6) and the linear equations (2) for each camera form a set of equations solved at every move applying Levenberg-Marquadt optimisation. The non-linear system is initialized with a Jacobian obtained by a linear method [16], converging after a few iterations. To obtain the enough number of equations to solve the equations system, the last realized moves method [16] was applied as well as a reliability factor [15]. Literature [5] [13] [14] [16] gathers several methods to estimate the Jacobian described by equation (2), we will describe that one gives the best results in order to be included into the tests. We must remark that a normalization of input data [8] (image points and articular increments) is carried out before calculation of the Jacobian in order to homogenize importance of each equation.

3.2 Recursive Least Squares (RLS) Method

In this method the Jacobian is estimated recursively by a least squares algorithm [1] [13], its equations are:

$$\mathbf{J}_k = \mathbf{J}_{k-1} + \frac{\left(-\Delta\mathbf{e}_k + \frac{\partial \mathbf{e}_k}{\partial t} \Delta t - \mathbf{J}_{k-1} \Delta\mathbf{q}_k \right) \Delta\mathbf{q}_k^T \mathbf{P}_{k-1}}{\lambda + \Delta\mathbf{q}_k^T \mathbf{P}_{k-1} \Delta\mathbf{q}_k} \tag{7}$$

where $\mathbf{e}_k = \mathbf{s}_k^* - \mathbf{s}_k$ is the image features error, and $\mathbf{s}_k^*$ the desired features, and

$$\mathbf{P}_k = \frac{1}{\lambda} \left(\mathbf{P}_{k-1} - \frac{\mathbf{P}_{k-1} \Delta\mathbf{q}_k \Delta\mathbf{q}_k^T \mathbf{P}_{k-1}}{\lambda + \Delta\mathbf{q}_k^T \mathbf{P}_{k-1} \Delta\mathbf{q}_k} \right) \tag{8}$$

is the covariance matrix. The behaviour of this method depends on the parameter λ, which varies in a range from 0 to 1, and ponders previous movements. λ settles a compromise between the information provided by old data from previous moves and new data, possibly corrupted by noise. In the presence of moderate noise, values of λ close to 0.9 are often used.

4 Analytic Image Jacobian

The analytic image Jacobian is given by [4]:

$$\mathbf{J}_A = \mathbf{J}_{sr}\mathbf{W}_{cr}\mathbf{N}\mathbf{J}_{rq} \tag{9}$$

where $\mathbf{J}_{rq}$ is the robot Jacobian, $\mathbf{N}$ is a matrix that contains the direct kinematic of the robot, $\mathbf{W}_{cr}$ is the relationship between kinematic screws of camera and robot given by:

$$\mathbf{W}_{cr} = \begin{bmatrix} \mathbf{R}_{cr} & [\mathbf{t}_{cr}]_x\mathbf{R}_{cr} \\ \mathbf{0}_3 & \mathbf{R}_{cr} \end{bmatrix} \tag{10}$$

being $\mathbf{R}_{cr}$ and $\mathbf{t}_{cr}$ rotation and translation respectively between camera and robot, $[\mathbf{t}_{cr}]_x$ is the skew-symmetric matrix of $\mathbf{t}_{cr}$, and $\mathbf{J}_{sr}$ is the interaction matrix given by (1).

As can be seen in (9), analytic Jacobian depends on several parameters and transforms that become it very dependent on their accuracy. Some of them are constants as the calibration of the cameras, and transform camera-robot, and others must be determined on line as the direct kinematic and the robot Jacobian.

5 Control Law

The task function $\mathbf{e}_k$ to be regulated to zero is given by:

$$\mathbf{e}_k = (\mathbf{s}^* - \mathbf{s}_k) \tag{11}$$

where $\mathbf{s}^*$ and $\mathbf{s}_k$ are vectors of desired and current features at moment k respectively.

A proportional control law based on the pseudoinverse of the Jacobian [2] [4] was used to control the system, where the exponential decay of $\mathbf{e}_k$ to 0 is obtained by imposing $\dot{\mathbf{e}}_k = -\lambda\mathbf{e}_k$ (being λ is a positive scalar that regulates the convergence rate), the corresponding control law for the static (positioning) case is:

$$\mathbf{q}_{k+1} = \mathbf{q}_k + \lambda\mathbf{J}^+\mathbf{e}_k \tag{12}$$

being $\mathbf{J}^{+} = \left(\mathbf{J}^{\mathrm{T}}\mathbf{J}\right)^{-1}\mathbf{J}^{\mathrm{T}}$ the pseudoinverse of the Jacobian, since there are more features than number of DOF. It is proved that (12) has local asymptotic stability [2].

For the dynamic (tracking) case, a predictive term is added based on the last and the next to the last reference [13]:

$$\mathbf{q}_{k+1} = \mathbf{q}_k + \mathbf{J}^{+}\left(\mathbf{s}_k^{*} - \mathbf{s}_k + \mathbf{s}_k^{*} - \mathbf{s}_{k-1}^{*}\right) \tag{13}$$

6 Experiments

In this section we describe our experimental equipment and results.

6.1 Experimental Setup

The system used in the experiments consists of:

- A joint system composed of a high precision positioning device and its controller, model Newport MM3000 (see Fig. 1). The system has 3 DOF: one prismatic and two revolute joints, and their theoretical precisions are of a thousandth of a millimeter and a thousandth of a degree. The visual control object, is made out of five black dots on a white background, the projection of which on the image will be the control features, has been attached to the last link of the joint system.
- An image acquisition and processing system composed by two CV-M50 analogic cameras and a Matrox Meteor II-MC image adquisition board, which allows simultaneous acquisition from both cameras. The cameras, fixed in the working environment, are separated by about 700 millimeters, their both axes converge towards the joint system, and they are separated from it by about 1200 millimeters. Visual features are detected with sub-pixel precision, and due to the simplicity of the image, the error is estimated to be of less than 0.2 pixels. Communication with the joint system controller is established through a serial RS-232C cable.

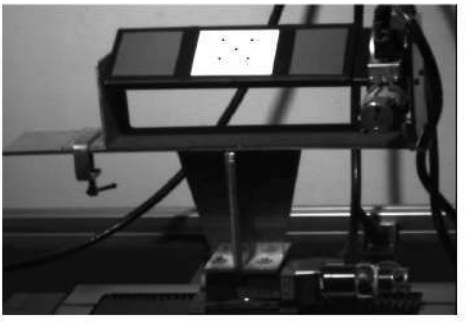

Fig. 1. Experimental setup

6.2 Control Objective

We intend to contrast the performance of two methods to estimate image Jacobian (FUNDMAT: by integrating epipolar restriction, RLS: by using recursive last square) and the analytic Jacobian (ANLTC) method, by means of static (positioning) and dynamic (tracking) tasks using the respective control law, where the number of points for controlling the system is taken into account. Likewise tests were carried out without added noise and with added noise (Gaussian noise $\sigma = 0.5$ pixel) in detecting features. Image features are centroids of projected points (Fig. 1). Visual features must be reachable and the visual object must be visible from both views. Due to the joint system only has 3 DOF, and to ensure coherence, we have obtained visual features for all desired positions previously from a teach-by-showing technique [11] where the joint system is moved to a desired position and its corresponding image features are recorded.

6.2.1 Static Case

Starting from an initial position, the system has to achieve consecutively desired features (Fig. 3, Fig.4, and Fig.5). A trajectory will be generated in both image plane and the joint space. If the error (Euclidean distance) between current and desired features is less than 0.6 pixels, it is meant that desired features have been reached. A high number of positions (up 50) obtained randomly in all over the workspace are linked in order to obtain more representative results.

6.2.2 Dynamic Case

The system has to follow image features belonging to a curve trajectory set in advance into the workspace (Fig. 7 and Fig. 8) built from random parameters. Similar to static case, in order to obtain more representative results, a high number of trajectories are generated into the workspace to be tracked.

6.3 Evaluation Indices

To evaluate the performance of methods to be evaluated, we consider two indices, defined as follows:

- Index 0: Sum of Euclidean distances between desired and current visual features. Weighted by number of considered points, number of cameras and number of desired positions.
- Index 1: Sum of Euclidean distances between desired and current joint positions. Weighted by number of considered points.

6.4 Results

A comparative study was conducted on the two methods of estimating image Jacobian (FUNDMAT, RLS) and the analytic method (ANLTC). Furthermore to prove the strong dependency of analytic Jacobian to parameters which have to be calculated on line or prior the control task, we have degraded some of them. In this way, tests were

also carried out with a degraded analytic Jacobian, we have degraded the depth Z of the point to be detected in about 3% and 5% (ANLTC z3%, ANLTC z5%) and the transform camera-robot $\mathbf{R}_{cr}$ and $\mathbf{t}_{cr}$ in about 3% and 4% (ANLTC W2%, ANLTC W3%). Increasing these levels of degradation, the system is no longer controlled. Additionally another test for ANLTC was considered: a constant depth equal to desired position as many authors do (ANLTC Zd) [2] [6].

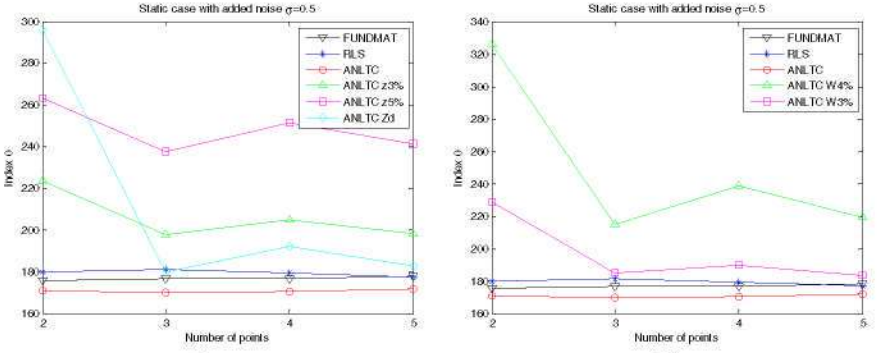

a) b)

Fig. 2. Index 0 for static case with added noise when a)degradation of depth Z is included. b)degradation of transform camera-robot is included

These two graphs show that for low levels of degradation in whether depth Z (Fig.2a) or transform camera-robot (Fig.2b), the behaviour of ANLTC is degraded. Results for without added noise are similar. Next graphs show the articular evolution (Fig.3, Fig.4, and Fig.5), red circles represent desired positions to be reached, and the blue line the evolution of the joint system.

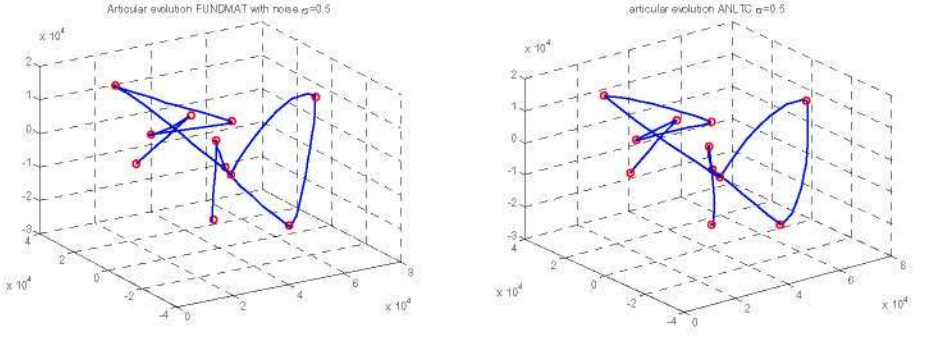

a) b)

Fig. 3. Evolution for ten desired position static case with noise: a)FUNDMAT, b)ANLTC

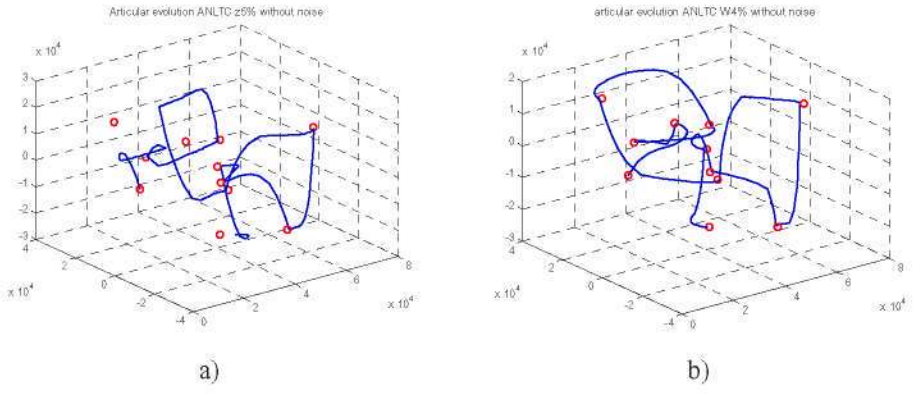

Fig. 4. Evolution for ten desired position static case without noise: a)ANLTC with degradation of depth Z 5%, b) ANLTC with degradation of transform camera-robot 4%

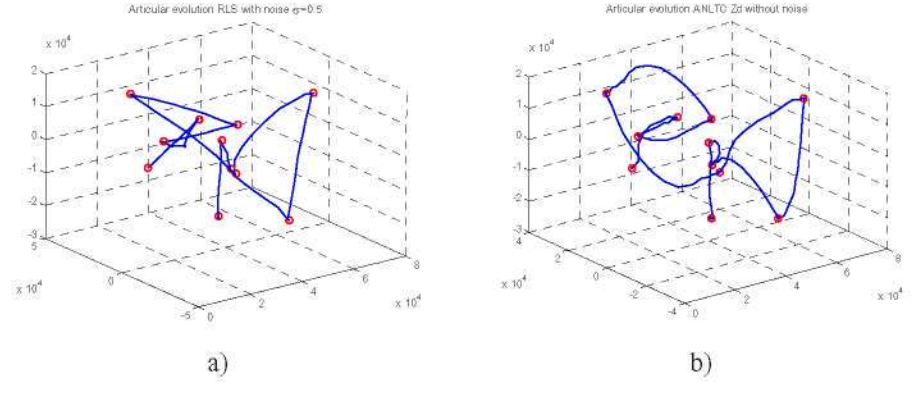

Fig. 5. Evolution for ten desired position static case: a)RLS with added noise, b) ANLTC Zd without noise

Fig.3a and Fig.3b show a good performance of FUNDMAT and ANLTC respectively (generated trajectory is almost direct even with added noise). Fig.4a and Fig.4b show an important degradation of the trajectory for ANLTC z5% and ANLTC W4% respectively even noise was not added. Trajectory of RLS (Fig 5a) with noise has not the same good behaviour as ANLTC and FUNDMAT (Fig.3). Trajectory of ANLTC Zd (Fig. 5b) has no good performance even without noise. Results for dynamic case are drawn in the following figures:

Fig.6 shows the same tendency as static case (Fig.2), furthermore it shows that RLS has less good behaviour than ANLTC and FUNDMAT. Fig.7 shows that ANLTC and FUNDMAT have good performance in articular evolution even the added noise.

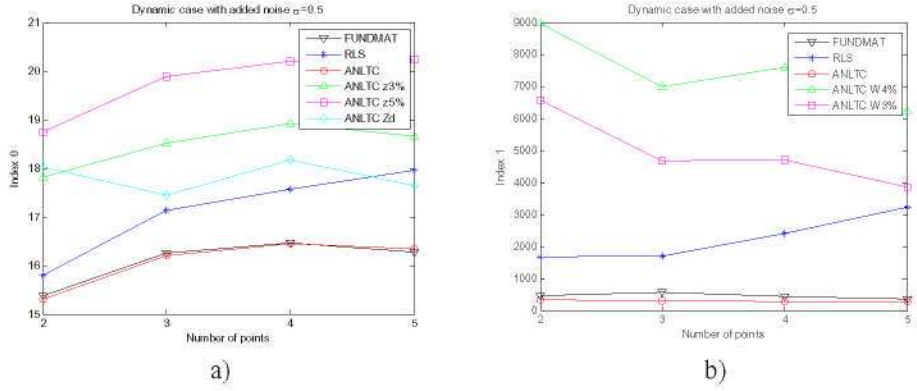

a) b)

Fig. 6. a)Index 0 for dynamic case with noise when degradation of depth Z is included. b)Index 1 for dynamic case with noise when degradation of transform camera-robot is included.

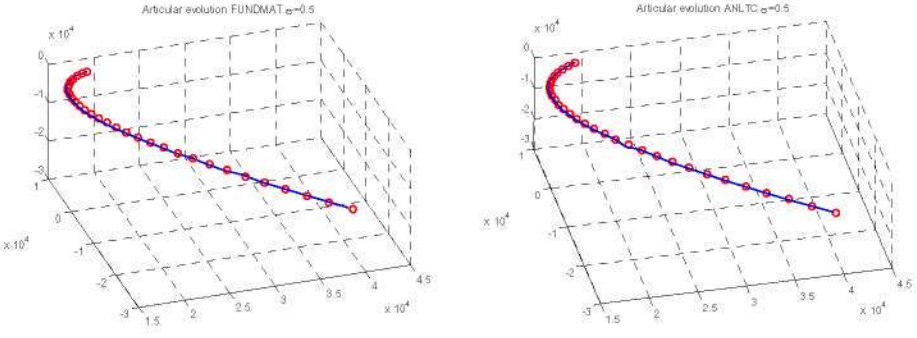

a) b)

Fig. 7. Articular evolution for dynamic case with noise: a)FUNDMAT, b)ANLTC

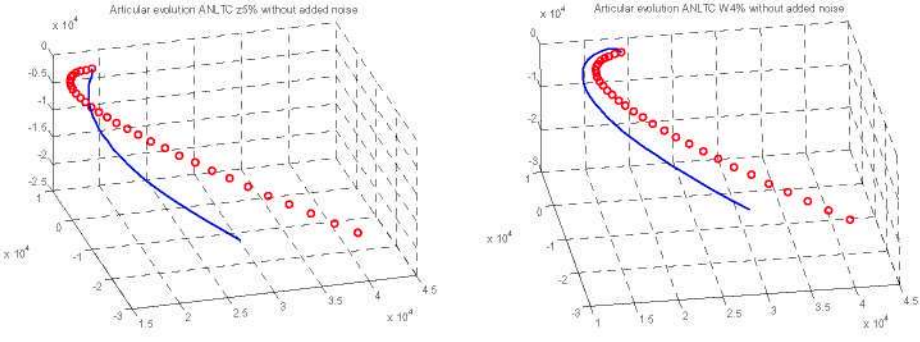

a) b)

Fig. 8. Articular evolution for dynamic case without noise: a)ANLTC with degradation of depth Z 5%, b) ANLTC with degradation of transformation camera-robot 4%

For dynamic case, Fig.8 also shows the degradation in articular evolution of the ANLTC behaviour as the static case (Fig.4 and Fig.5b) even without added noise. Moreover, tests with noise showed the same behaviour as Fig.8, in this way, it means that these levels of degradation affect to the behaviour stronger than added noise. It was observed that the last statement is also true for the static case.

7 Conclusion

A performance comparison has been carried out between a control task that comes from the estimation of the image Jacobian (represented by FUNDMAT that integrates the fundamental matrix and RLS: the recursive least square method) and that one that comes from a calculation (ANLTC: analytic Jacobian method). Tests have shown that in absence of noise, behavior of these three methods work quite similar. But in tests with added noise, FUNDMAT and ANLTC showed to be very robust. Analytic Jacobian works well, but at the expense of doing laborious previous work to the control task, it needs the camera calibration, 3D reconstruction of the point, the transformation camera-robot, and the robot Jacobian. Tests with whether degradation of camera-robot transform or depth of the detected point showed that the performance of analytic Jacobian is degraded even for low values of degradation.

Considering the good performance of the method that estimates the image Jacobian by integrating the fundamental matrix (FUNDMAT) and the fact that this method does not need previous work to the control task in contrast to the analytic Jacobian does, it is considered as an important advantage. This fact becomes it to be appropriate for tasks in unknown or changing environments because the knowledge of the fundamental matrix is not an objection, and its calculation has been proven to be much more simple, robust and reliable. The future work is the analysis of the system stability with the control law generated from the estimated Jacobian.

This work was supported by the Comisión Interministerial de Ciencia y Tecnología of the Spanish Government under the Project DPI2004-07433-C02-02.

References

[1] Asada, M., Tanaka, T., Hosoda, K.: Adaptive Binocular Visual Servoing for Independently Moving Target Tracking. In: Proceedings of the IEEE International Conference on Robotics and Automation (ICRA 2000), pp. 2076–2081 (2000)

[2] Chaumette, F., Hutchinson, S.: Visual Servo Control Part I: Basic Approaches. IEEE Robotics & Autonomation Magazine 14(1), 109–118 (2006)

[3] Chaumette, F., Hutchinson, S.: Visual Servo Control Part II: Advanced Approaches. Robotics & Autonomous Magazine, IEEE 13(4), 82–90 (2007)

[4] Corke, P.: Visual Control of Robot Manipulators – A Review. In: Hashimoto, K. (ed.) Visual Servoing, pp. 1–32. World Scientific, Singapore (1994)

[5] Deng, Z., Jägersand, M.: Evaluation of Model Independent Image-Based Visual Servoing. In: Canadian Conference on Computer and Robot Vision, pp. 138–144 (2004)

[6] Espiau, B., Chaumette, F., Rives, P.: A New Approach to Visual Servoing in Robotics. IEEE Transactions on Robotics and Automation 8(3), 313–326 (1992)

[7] Faugeras, O., Luong, Q.T.: The Geometry of Multiple Images. The Massachusetts Institute of Technology Press (2001)
[8] Hartley, R.I.: In Defence of the Eight-Point Algorithm. IEEE Transactions on Pattern Analysis and Machine Intelligence 19(6) (1997)
[9] Hartley, R., Zisserman, A.: Multiple View Geometry in Computer Vision, 2nd edn. Cambridge University Press, Cambridge (2003)
[10] Hutchinson, S.A., Hager, G.D., Corke, P.I.: A tutorial on visual servo control. IEEE Trans. Robotics and Automation 12, 651–670 (1996)
[11] Kragic, D., Christensen, H.I.: Survey on visual servoing for manipulation, Technical Report ISRN KTH/NA/P-02/01-Sen, CVAP259, (2002)
[12] Pari, L., Sebastián, J.M., González, C., Ángel, L.: Image Based Visual Servoing: A New Method for the Estimation of the Image Jacobian in Dynamic Environments. In: Campilho, A., Kamel, M. (eds.) ICIAR 2006. LNCS, vol. 4142, pp. 850–861. Springer, Heidelberg (2006)
[13] Piepmeier, J.A., McMurray, G.V., Lipkin, H.: Uncalibrated Dynamic Visual Servoing. IEEE Transactions on Robotics and Automation 20(1), 143–147 (2004)
[14] Qian, J., Su, J.: Online estimation of Image Jacobian Matrix by Kalman-Bucy filter for un-calibrated Stereo Vision Feedback. In: International Conference on Robotics & Automation (ICRA 2002), pp. 562–567 (2002)
[15] Sebastián, J.M., Pari, L., González, C., Ángel, L.: A New Method for the Estimation of the Image Jacobian for the Control of an Uncalibrated Joint System. In: Marques, J.S., Pérez de la Blanca, N., Pina, P. (eds.) IbPRIA 2005. LNCS, vol. 3522, pp. 631–638. Springer, Heidelberg (2005)
[16] Sutanto, H., Sharma, R., Varma, V.: The role of exploratory movement in visual servoing without calibration. Robotics and Autonomous Systems 23, 153–169 (1998)